Oscillations and variability in the p53 system, Geva-Zatorsky et al. 2006

Supplementary figure and movie legends

Figure S1. An example of a field of view with several cells (in bright field illumination, gray) overlaid by the fluorescence intensities of p53-CFP and Mdm2-YFP (shown in green and red respectively, their overlap is seen in yellow).

Figure S2. Nuclear Mdm2-YFP dynamics of all the measured cells in a single movie exposed to A) 10Gy, and B) no gamma irradiation. Dotted vertical lines indicate division events; solid vertical lines indicate severe blebbing of the cell's membrane. C) Timing of nuclear Mdm2-YFP dynamics in oscillating cells exposed to 10Gy of gamma irradiation (see Fig. 2D). Blue hues indicate low fluorescence levels and yellow-reddish colors indicate high fluorescence levels. Dotted lines show 6 hour intervals. D) Timing of Mdm2-YFP fluctuations in cells not exposed to gamma irradiation. E) Mdm2-YFP dynamics averaged over all cells exposed to 10Gy (solid blue line) and to no gamma irradiation (dotted black line).

Figure S3. Power spectrum of nuclear Mdm2-YFP fluorescence dynamics in individual cells. Top: an example of a cell showing fluctuations with a characteristic frequency of ~10 hours (exposed to 0.3Gy of gamma irradiation), and the power spectrum of the signal (by Fourier transform). Bottom: an example of a cell with multiple oscillations with a period of ~6 hours (exposed to 5Gy), and the power spectrum of the signal (right).

Figure S4. Examples of cells (following 5Gy of gamma irradiation) showing continuous Mdm2-YFP oscillations, some of whose peaks have no detectable corresponding p53-CFP peaks. Detectable peaks show a large variation in amplitude.

Figure S5. Average amplitude and width of the first five p53-CFP oscillation peaks in cells exposed to different doses of gamma irradiation, shown with their standard errors. Left: average oscillation amplitude of each of the first 5 peaks. Right: Average width of each of the first 5 peaks. Measurements include data from 146, 163, and 128 cells after 5, 2.5, and 0.3 Gy of gamma irradiation, respectively.

Figure S6. An averaged oscillation pattern used for comparison to deterministic simulations of models. This pattern was meant to resemble an idealized undamped oscillation with peak characteristics that correspond to the average peak characteristics of oscillating cells. Note

that this pattern is different from the damped oscillations that result when averaging the dynamics of many cells due to the lack of precise synchrony in the oscillations. Cells which exhibit 2 peaks in the first 16 hours were collected, and the first and second peaks were identified between the consecutive minima. Each peak was normalized to the average peak maximum and shifted in time so that its maximum coincides with the average peak timing. The average shape for each pulse was calculated by averaging the normalized peaks, and the two peaks were smoothly linked. The second peak was duplicated at equal intervals to get a continuous signal.

Figure S7. Generation of time-dependent noise. Left: for every central frequency, a Gaussian wave packet of amplitudes was constructed with varying widths. Right: a time-dependent signal $\eta(t)$ was calculated by summing the component frequencies with random phases, obtaining a signal with a mean~0, and normalizing its STD to a given value. The multiplicative noise factor that was used was $\xi(t)=\exp(\eta(t))$.

Figure S8. Sensitivity of models to variations in parameters. For each of the oscillating models II-VI, every parameter was varied from 0.1 times to 10 times its best-fit value (Table 1). Dynamics were simulated and peaks were identified. The median value of the p53 (green) and Mdm2 (red) maxima, and the oscillation period (black) were calculated. These values were then divided by the best-fit values, to obtain the relative change. Blue stars mark parameters that significantly changed the amplitude but did not affect the period of the oscillations (by more than ~10%). Lack of data points in certain panels indicate that no oscillations occurred for the respective parameter values.

Figure S9. Diagrams and simulations for model VI. In these simulations the system was allowed to stabilize to its steady state without damage (for $t<0$, $\theta(Damage)=0$ or $\beta_S=0$) and damage was induced at time $t=0$ (for $t>0$, $\theta(Damage)=1$). A) The simplified form (model VI in main text) simulated with parameter values in table I. B) A more detailed formulation which includes both *active* and *inactive* species of p53, and an *inhibitor* of *Signal* separate from *Mdm2* (see appendix I). Simulation uses the same parameter values, $T_S=1$, $\beta_{p53}=\beta_x$, $\beta_{inhibitor}=\beta_{Mdm2}=\beta_y$, $\beta_{Signal}=\beta_S$, $\alpha_{Signal}=\alpha_S$, $\alpha_{inhibitor}=\alpha_{Mdm2}=\alpha_y$, with $\alpha_{active}=\alpha_{xy}$, $\alpha_{inactive}=100\cdot\alpha_{active}$, $\omega=500\cdot\alpha_{active}$, and $\tau=80$. C) An "Mdm2-centric" formulation which includes both *regular* and *modified* species of Mdm2 and an *inhibitor* of *Signal* (see appendix I). Simulations use the same parameters as (B), with $\alpha_{modified}=\alpha_{xy}$, $\alpha_{regular}=100\cdot\alpha_{modified}$, $\omega=100\cdot\alpha_{modified}$, and $\tau=120$.

Movie Geva-Zatorsky2006_SM1.mpg: A time-lapse movie of one cell nucleus (shown in Fig. 1AB), after exposure to a 5Gy gamma dose. The normalized dynamics of p53-CFP (in green) and Mdm2-YFP (in red) are plotted on the right.

Supplementary text

Appendix I: Biologically motivated expanded formulations of model VI.

The core models (Fig. 6A), with the 3 dynamic variables, can be readily extended to encompass other important aspects of the p53 system. For example, a recently published model for p53-Mdm2 oscillations (Ma et al., 2005; Wagner et al., 2005) can be compared to model IV or to model III (Wagner et al., 2005). Here we present two examples of expanded forms of model VI. In the first example (Fig. S9B), two forms of p53 are explicitly included in the model. Without DNA damage, p53 exists in the inactive form, $p53_{inactive}$. The transcription rate of p53 has been shown to be independent of DNA damage (Haupt et al., 1997; Vassilev, 2004). Evidence was presented for an increase in translation rate of p53 following gamma irradiation (Fu and Benchimol, 1997), an effect that can contribute to the oscillatory properties. In order to maintain simplicity in the models we represent production of p53 by a constant rate β_{p53}. The degradation rate of p53 can depend on numerous factors, including Mdm2. Following DNA damage, *Signal*, *S*, is activated (perhaps representing phosphorylated ATM (Bakkenist and Kastan, 2003)). When *S* accumulates ($S>T_s$), it modifies inactive p53 ($p53_{inactive}$) converting it into its active form, $p53_{active}$ (Appella and Anderson, 2001; Unger et al., 1999), at a rate ω. *Mdm2* promotes the degradation of p53 (Haupt et al., 1997; Kubbutat et al., 1997). The production rate of Mdm2 is enhanced by p53 (Barak et al., 1993; Wu et al., 1993). Active p53, has a weaker interaction with Mdm2 than inactive p53 and hence a lower degradation rate, $\alpha_{active}<\alpha_{inactive}$ (Shieh et al., 1997). Thus, activation of p53 leads to its accumulation, and as its levels increase, this increases the production rate of Mdm2. Because of the accumulation of active p53, the same results are obtained by the model whether the downstream genes are induced by active p53 alone or by both varieties ($p53_{active}$+$p53_{inactive}$). In the transactivation terms of downstream genes we therefore use *p53* (without subscript) to denote either of these options. The increased Mdm2 levels in the nucleus lead to faster degradation (or nuclear export) of $p53_{active}$. After levels of p53 drop in the nucleus, the production rate of Mdm2 decreases and it is degraded (or exported out of the

nucleus) back to low level. The *inhibitor* of *Signal* (a putative interaction included in this model but not in the other models I-V) follows dynamics which are similar to those of *Mdm2*, so that *Signal* is inhibited during the pulse but this inhibition is removed when the pulse ends and levels of *inhibitor, I*, drop. The equations for such a model can be written as follows: ($\theta(Damage)$ is equal to 1 if damage exists, zero otherwise; *p53* represents either $p53_{active}$ or the sum of both species)

$$\frac{d}{dt}p53_{inactive} = \beta_{p53} - \alpha_{inactive} \cdot Mdm2 \cdot p53 - \omega \cdot \frac{S^n}{S^n + T_S} \cdot p53_{inactive}$$

$$\frac{d}{dt}p53_{active} = \omega \cdot \frac{S^n}{S^n + T_S} \cdot p53_{inactive} - \alpha_{active} \cdot Mdm2 \cdot p53_{active}$$

$$\frac{d}{dt}Mdm2 = \beta_{Mdm2} \cdot p53(t-\tau) - \alpha_{Mdm2} \cdot Mdm2$$

$$\frac{d}{dt}I = \beta_{inhibitor} \cdot p53(t-\tau) - \alpha_{inhibitor} \cdot I$$

$$\frac{d}{dt}S = \beta_{Signal} \cdot \theta(Damage) - \alpha_{Signal} \cdot I \cdot S$$

For fast modification rates of p53 (large ω, $\omega >> \alpha_{active}$), with the parameters for the inhibitor equal to the values for Mdm2, the dynamics obtained by this model are equivalent to those obtained by the simplified model VI (Fig. S8A). The inhibitor could be either Mdm2 itself or a different component with similar dynamic properties. *Signal* thus oscillates, with a shifted phase, such that *Signal* peaks precede the p53 peaks, and are in an opposite phase to p53-downstream genes such as Mdm2 and possibly DNA repair genes. This can create a separation of phases where DNA damage sensing (by *Signal*) and activity of p53-downstream genes are separated in time. Note that other reported negative feedbacks on p53, such as the feedback through COP1 (Dornan et al., 2004) or Pirh2 (Leng et al., 2003), can be introduced into this model by duplicating the equation for Mdm2 and modifying the interaction parameters to maintain the same dynamic profile for p53 and Mdm2. It would be interesting to examine whether these components of the p53 system do indeed oscillate and whether their dynamics can indeed be modeled in this same fashion.

An alternative formulation places an emphasis on the role of Mdm2 in regulating the p53 response (see reviews in (Bond et al., 2005; Momand et al., 2000)), through varied Mdm2 levels (Stommel and Wahl, 2004), covalent modifications (Maya et al., 2001), or binding of other components such as Arf (Zhang and Xiong, 2001). In this formulation, Mdm2 protein exists in two distinct forms, so that following irradiation and DNA damage the "regular", unmodified form of Mdm2 (denoted $Mdm2_{regular}$) becomes modified ($Mdm2_{modified}$). The

modified form of Mdm2 has a weaker interaction with p53, with $\alpha_{modified}<\alpha_{regular}$. The equations would then have the form:

$$\frac{d}{dt}p53 = \beta_{p53} - \alpha_{regular}\cdot Mdm2_{regular}\cdot p53 - \alpha_{\mathrm{mod}\,ified}\cdot Mdm2_{\mathrm{mod}\,ified}\cdot p53$$

$$\frac{d}{dt}Mdm2_{regular} = \beta_{Mdm2}\cdot p53(t-\tau) - \alpha_{Mdm2}\cdot Mdm2_{regular} - \omega\cdot\frac{S^n}{S^n+T_S}\cdot Mdm2_{regular}$$

$$\frac{d}{dt}Mdm2_{\mathrm{mod}\,ified} = \omega\cdot\frac{S^n}{S^n+T_S}\cdot Mdm2_{regular} - \alpha_{Mdm2}\cdot Mdm2_{\mathrm{mod}\,ified}$$

$$\frac{d}{dt}I = \beta_{inhibitor}\cdot p53(t-\tau) - \alpha_{inhibitor}\cdot I$$

$$\frac{d}{dt}S = \beta_{Signal}\cdot\theta(Damage) - \alpha_{Signal}\cdot I\cdot S$$

Again, for fast modification rates (large ω, $\omega>>\alpha_{modified}$), the dynamics obtained by this model (Fig. S8C) are equivalent to those obtained by the model above and by the simplified model VI (Fig. S8AB).

Different formulations of the model may be relevant for comparison to different experimental settings and manipulations. One could further expand these to include multiple forms of p53, Mdm2, and other components, and the dynamic properties and response to noise would be preserved, as long as the model maintains its homology to model VI. Such variants of the model can be distinguished by measuring the dynamics of modified components or their interactions, or through the effects of mutations (Bond et al., 2004) or drugs (Vassilev, 2004) on the oscillations. The important distinction between these variants and other models of the p53-Mdm2 feedback (models I-V) is the different connectivity which includes a second, longer negative feedback loop, by inhibition of damage signaling through p53-downstream factors (e.g. *inhibitor*). Although much evidence has been accumulated for signaling of damage to p53 (Lee and Paull, 2005; Stommel and Wahl, 2004), the feedback from p53 and Mdm2 back to the damage signal is an unknown interaction predicted by this model.

References to supplementary text

Appella, E., and Anderson, C. W. (2001). Post-translational modifications and activation of p53 by genotoxic stresses. Eur J Biochem *268*, 2764-2772.

Bakkenist, C. J., and Kastan, M. B. (2003). DNA damage activates ATM through intermolecular autophosphorylation and dimer dissociation. Nature *421*, 499-506.

Barak, Y., Juven, T., Haffner, R., and Oren, M. (1993). mdm2 expression is induced by wild type p53 activity. Embo J *12*, 461-468.

Bond, G. L., Hu, W., Bond, E. E., Robins, H., Lutzker, S. G., Arva, N. C., Bargonetti, J., Bartel, F., Taubert, H., Wuerl, P., *et al.* (2004). A Single Nucleotide Polymorphism in the MDM2 Promoter Attenuates the p53 Tumor Suppressor Pathway and Accelerates Tumor Formation in Humans. Cell *119*, 591-602.

Bond, G. L., Hu, W., and Levine, A. J. (2005). MDM2 is a central node in the p53 pathway: 12 years and counting. Curr Cancer Drug Targets *5*, 3-8.

Dornan, D., Wertz, I., Shimizu, H., Arnott, D., Frantz, G. D., Dowd, P., O'Rourke, K., Koeppen, H., and Dixit, V. M. (2004). The ubiquitin ligase COP1 is a critical negative regulator of p53. Nature *429*, 86-92.

Fu, L., and Benchimol, S. (1997). Participation of the human p53 3'UTR in translational repression and activation following gamma-irradiation. Embo J *16*, 4117-4125.

Haupt, Y., Maya, R., Kazaz, A., and Oren, M. (1997). Mdm2 promotes the rapid degradation of p53. Nature *387*, 296-299.

Kubbutat, M. H., Jones, S. N., and Vousden, K. H. (1997). Regulation of p53 stability by Mdm2. Nature *387*, 299-303.

Lee, J. H., and Paull, T. T. (2005). ATM activation by DNA double-strand breaks through the Mre11-Rad50-Nbs1 complex. Science *308*, 551-554.

Leng, R. P., Lin, Y., Ma, W., Wu, H., Lemmers, B., Chung, S., Parant, J. M., Lozano, G., Hakem, R., and Benchimol, S. (2003). Pirh2, a p53-induced ubiquitin-protein ligase, promotes p53 degradation. Cell *112*, 779-791.

Ma, L., Wagner, J., Rice, J. J., Hu, W., Levine, A. J., and Stolovitzky, G. A. (2005). A plausible model for the digital response of p53 to DNA damage. Proc Natl Acad Sci U S A *102*, 14266-14271.

Maya, R., Balass, M., Kim, S. T., Shkedy, D., Leal, J. F., Shifman, O., Moas, M., Buschmann, T., Ronai, Z., Shiloh, Y., *et al.* (2001). ATM-dependent phosphorylation of Mdm2 on serine 395: role in p53 activation by DNA damage. Genes Dev *15*, 1067-1077.

Momand, J., Wu, H. H., and Dasgupta, G. (2000). MDM2-master regulator of the p53 tumor suppressor protein. Gene *242*, 15-29.

Shieh, S. Y., Ikeda, M., Taya, Y., and Prives, C. (1997). DNA damage-induced phosphorylation of p53 alleviates inhibition by MDM2. Cell *91*, 325-334.

Stommel, J. M., and Wahl, G. M. (2004). Accelerated MDM2 auto-degradation induced by DNA-damage kinases is required for p53 activation. Embo J *23*, 1547-1556.

Unger, T., Juven-Gershon, T., Moallem, E., Berger, M., Vogt Sionov, R., Lozano, G., Oren, M., and Haupt, Y. (1999). Critical role for Ser20 of human p53 in the negative regulation of p53 by Mdm2. Embo J *18*, 1805-1814.

Vassilev, L. T. (2004). Small-molecule antagonists of p53-MDM2 binding: research tools and potential therapeutics. Cell Cycle *3*, 419-421.

Wagner, J., Ma, L., Rice, J. J., Hu, W., Levine, A. J., and Stolovitzky, G. A. (2005). p53-Mdm2 loop controlled by a balance of its feedback strength and effective dampening using ATM and delayed feedback. IEE Proc-Syst Biol *152*, 109-118.

Wu, X., Bayle, J. H., Olson, D., and Levine, A. J. (1993). The p53-mdm-2 autoregulatory feedback loop. Genes Dev *7*, 1126-1132.

Zhang, Y., and Xiong, Y. (2001). Control of p53 ubiquitination and nuclear export by MDM2 and ARF. Cell Growth Differ *12*, 175-186.

Geva-Zatorsky et al. 2006, supplementary figures

Fig. S1

Geva-Zatorsky et al. 2006, supplementary figures

Fig. S2

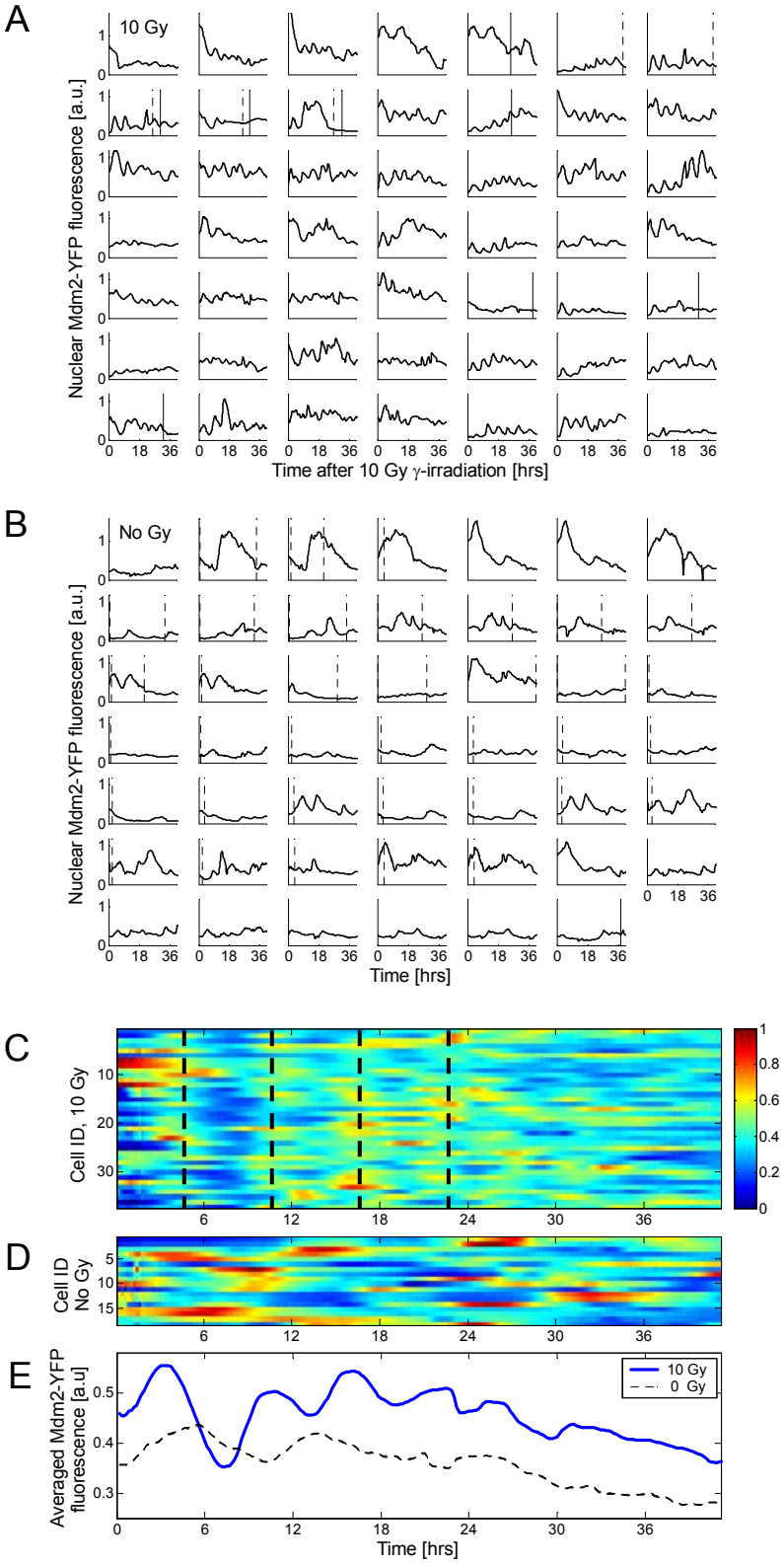

Geva-Zatorsky et al. 2006, supplementary figures

Fig. S3

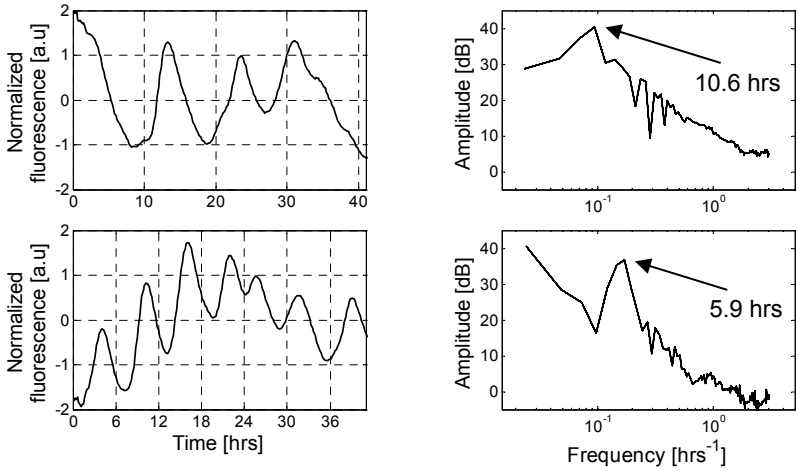

Fig. S4

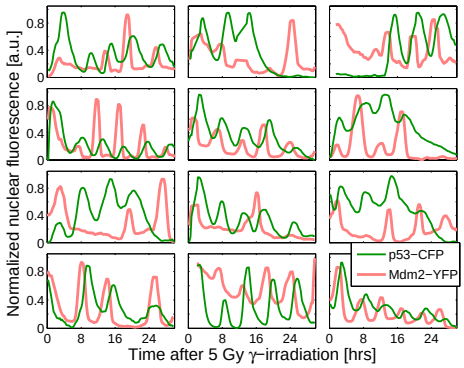

Fig. S5

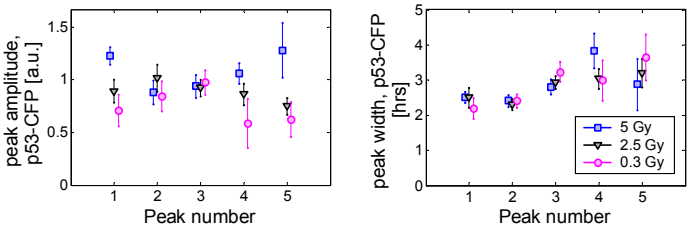

Fig. S6

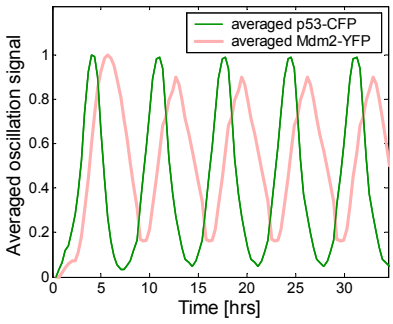

Fig. S7

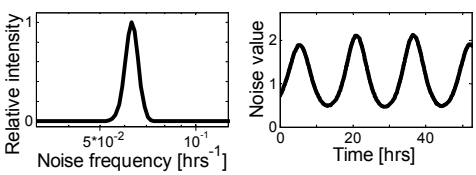

Geva-Zatorsky et al. 2006, supplementary figures

Fig. S8

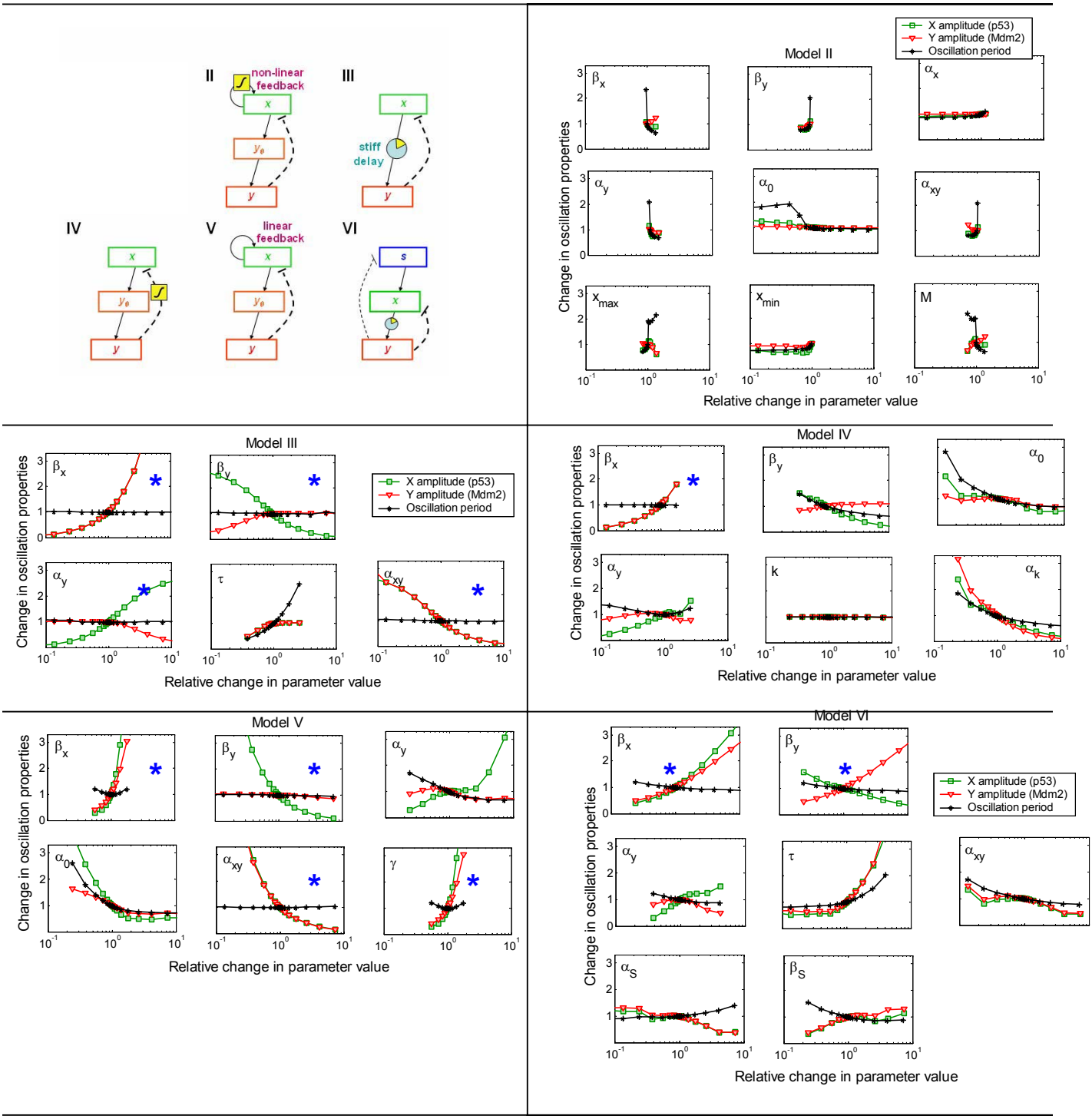

Geva-Zatorsky et al. 2006, supplementary figures

Fig. S9

A

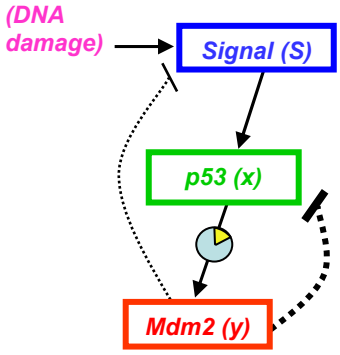

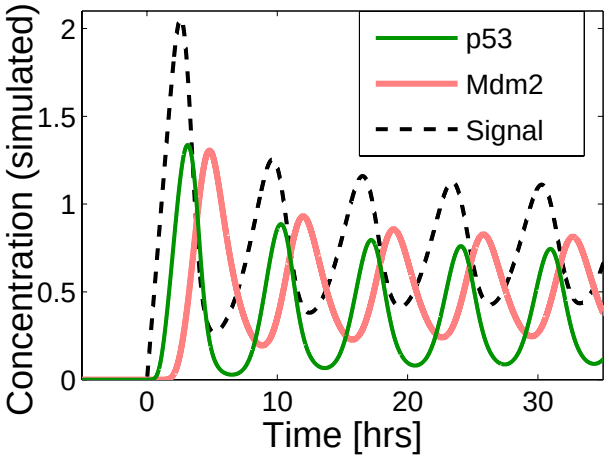

B

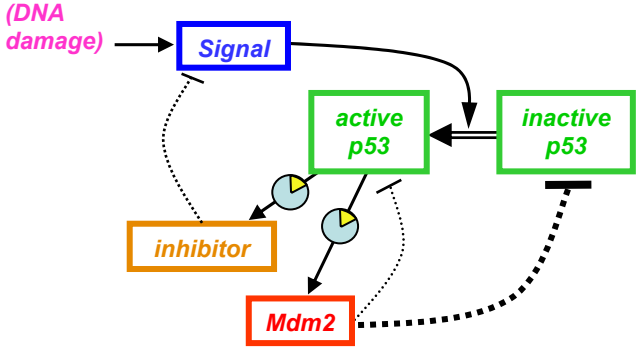

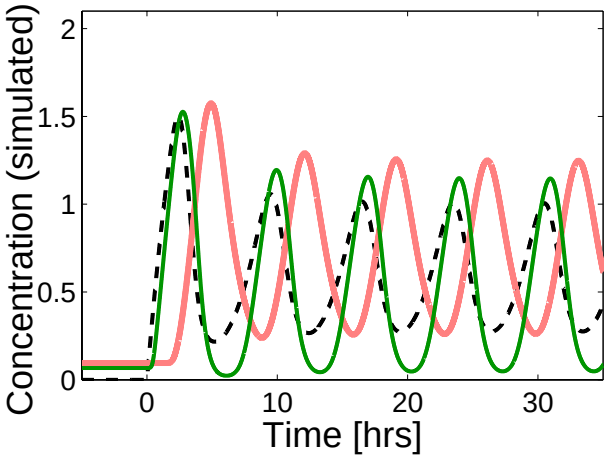

C